Available online at www.sciencedirect.com
ScienceDirect
Journal of Power Sources 171 (2007) 953–959
JOURNAL OF POWER SOURCES
www.elsevier.com/locate/jpowsour

Electrochemical recycling of cobalt from cathodes of spent lithium-ion batteries

M.B.J.G. Freitas *, E.M. Garcia

Universidade Federal do Espírito Santo, Departamento de Química, Laboratório de Eletroquímica Aplicada, Av. Fernando Ferrari 514, Goiabeiras, Vitória, ES CEP: 29070-910, Brazil

Received 17 April 2007; received in revised form 30 June 2007; accepted 3 July 2007
Available online 10 July 2007

Abstract

In this work, cobalt from spent cellular telephone Li-ion batteries was recovered by electrochemical techniques. According to X-ray diffraction results, the composition of the positive electrode is $LiCoO_2$, Co_3O_4, C, and Al. The largest charge efficiency found was 96.90% at pH 5.40, potential applied of −1.00 V and a charge density of 10.0 °C cm^{-2}. The charge efficiency in the electrochemical recycling of cobalt decreases with the decrease in pH. The energy dispersive X-ray analysis (EDX) measurements of the electrodeposits showed that the surface is constituted of 100% cobalt. Scanning electron microscopy (SEM) showed a three-dimensional nucleus growth.

The application of nucleation models to the initial stages of electrodeposit growth shows that at pH 5.40 electrodeposition happens with progressive nucleation. With the decrease in pH to 2.70, nucleation becomes instantaneous.

Keywords: Li-ion batteries; Cobalt; Cobalt electrodeposition

1. Introduction

Li-ion batteries were first produced by Sony in 1991. These batteries have substituted Ni–Cd and Ni–MH batteries in many applications due to their high energy density, low auto-discharge rate, and excellent cycle life. Besides, are acceptable in environmental terms [1]. $LiCoO_2$ is the most used material in Li-ion battery cathodes due to its good performance [1]. Initial studies on Li_xCoO_2 showed that three phase transitions exist in the range $0.30 \leq x \leq 1.00$. A fourth irreversible phase appears for x smaller than 0.30. $Ni_{(x)}Co_{(1-x)}LiO_2$ is also used as an active material to avoid structural changes [2]. Aqueous electrolytes are not used in these batteries due to their high operation potential. Propylene carbonate and ethylene carbonate associated to inorganic lithium salts as either $LiPF_6$ or $LiClO_4$ are used as electrolytes [3,4]. The latter is little used due to its explosiveness. The main advantages of lithium ions are their reduced size and high thermodynamic potential, which facilitates their insertion into solid hosts with good intercalation and deintercalation kinetics. The anodic material used in Li-ion batteries is carbon. Li-ion batteries operate by reversible transport from an electrode to another [5]. The charge and discharge processes of batteries with $LiCoO_2$ as a cathode are represented by Eq. (1):

$$LiCoO_2 + C_6 \underset{\text{Discharge}}{\overset{\text{Charge}}{\rightleftharpoons}} Li_{(1-x)}CoO_2 + Li_xC_6 \quad (1)$$

The world production of Li-ion batteries in 2000 reached 500 million units and can to reach 4.6 billion in 2010 [6]. The use of portable devices, such as cellular telephones and microcomputers has contributed to their increased consumption. The residue generated by these batteries amounts to 500 thousand tonnes. About 5.0–15% of this residue is composed of cobalt present in the cathode. The cobalt quotation rose from US$ 20 to US$ 40 per kilogram between 1998 and 2002 [6]. In this scenery, it is necessary to recycle the positive electrode of these batteries. The electrochemically recovered cobalt may be used to make either alloys with magnetic properties or new electrodes [7]. The solution composition influences the cobalt electrodeposition mechanism and the deposit morphology directly. Several mechanisms are proposed for the reduction of cobalt [8–14]. At pH below 4.00, electrodeposition occurs through an unstable intermediate with the reduction of adsorbed CoH to metallic

* Corresponding author. Tel.: +55 27 33352486; fax: +55 27 33352460.
E-mail address: marcosbj@hotmail.com (M.B.J.G. Freitas).

0378-7753/$ – see front matter © 2007 Elsevier B.V. All rights reserved.
doi:10.1016/j.jpowsour.2007.07.002

cobalt and the adsorption of hydrogen. At pH above 4.00, the reaction happens with the initial formation of $Co(OH)_2$, which is then reduced to metallic cobalt [14–16].

In the present work, an electrochemical recycling method of cobalt from positive electrodes of spent Li-ion batteries using potentiostatic and potentiodynamic techniques was developed. The relationship between current density, charge efficiency, and deposit morphology was analyzed.

2. Experimental

2.1. Material characterization

The cathode and anode of spent Li-ion batteries were characterized by X-ray diffraction, SEM and EDX. The electrodeposits were characterized by SEM and EDX. In the leaching solutions were made measured of atomic absorption spectroscopy (AAS) to detect the presence of lithium, copper and cobalt.

The cobalt and lithium concentrations were equal to $0.10\,mol\,l^{-1}$, respectively. The ionic copper concentration was equal to $1.57 \times 10^{-7}\,mol\,l^{-1}$. That concentration is very low to influence the eletrodeposition process. The ionic lithium does not influence the cobalt electrodeposition because its reduction occurs in more cathodic potential (−3.02 V).

Atomic absorption spectroscopy measurements were accomplished in an AAS model AA-1275A from Intralab. X-ray measurements were accomplished in 200 B Rotaflex-Rigaku with copper Kα radiation, Ni filter, and scan speed of $2^\circ\,min^{-1}$. SEM and EDX measurements were accomplished in JEOL JXA model 8900 RL equipped with an energy dispersive X-ray detector.

2.2. Preparation of electrodeposition solutions

Li-ion batteries were manually dismantled and physically separated into their different parts: anode, cathode, steel, separators, and current collectors. The electrodes were dried at 80 °C for 24 h, and washed in distilled water at 40 °C for 1 h under agitation to eliminate organic solvents, propylene carbonate (PC) and ethylene carbonate (EC), and to facilitate the detachment of the active material from the respective current collectors. The active material was filtered and washed with distilled water at 40 °C to remove possible lithium salts, such as $LiPF_6$ and $LiCl_4$ and dried in air for 24 h. A mass of 9.17 g of positive electrodes was dissolved in a solution containing 470.00 ml of HCl $3.00\,mol\,l^{-1}$ and 30.00 ml H_2O_2 30% (v/v).

The system was maintained under constant magnetic agitation at 80 °C for 2 h. The cathode dissolution efficiency increases with the increase of the acid concentration and temperature. The addition of H_2O_2 is necessary to increase the efficiency of cathode dissolution [16,17]. H_2O_2 reduces cobalt from oxidation state +III, insoluble in aqueous system, to +II, soluble in aqueous system. Considering that the active material is $LiCoO_2$, the cathode dissolution reaction is represented by Eq. (2):

$$LiCoO_{2(s)} + \tfrac{1}{2}H_2O_{2(l)} + 3HCl_{(aq)} \rightarrow CoCl_{2(aq)} + \tfrac{1}{2}O_{2(g)} + LiCl_{(aq)} + 2H_2O_{(l)} \quad (2)$$

The pH of the leaching solution was adjusted with NaOH pellets to 1.5, 2.0, 2.7, 4.0, and 5.40. The solutions were buffered with H_3BO_3 $0.10\,mol\,l^{-1}$ to maintain constant the pH of electrodeposition bath. The pH of the bath has influences in the efficiency and morphology of electrodeposits as showed in item 3.3. Solutions without cobalt were prepared with H_3BO_3 $0.10\,mol\,l^{-1}$ and with support electrolyte Na_2SO_4 $0.10\,mol\,l^{-1}$ and LiCl $0.10\,mol\,l^{-1}$ at pH 5.40.

2.3. Electrochemical measurements

Electrochemical measurements were made using a power supply model MQPG-01 from Microchemistry. The working electrode was made of Al 99% (MERCK) and prepared as a rectangular foil with geometric area of $0.40\,cm^2$. The auxiliary electrode, with area of $3.75\,cm^2$, was made of platinum. The reference electrode was saturated Ag/AgCl/NaCl. The working electrodes were sanded with 600-grit sandpaper before each measurement and washed with distilled water. In the potentiodynamic measurements the initial and final potential polarization were −0.70 and −1.50 V. The potential scan rate was of $10.00\,mV\,s^{-1}$. Potentiostatic measurements were made applying potentials for cobalt reduction of: −0.80, −0.90, −1.00, −1.10, and −1.20 V. The charge density (Q) applied in each potential reduction was of $10.0\,C\,cm^{-2}$. The charge efficiency (α) was calculated using the Faraday law. The electrodeposits formed in potentiostatic condition were dissolved in a H_2SO_4 $0.50\,mol\,l^{-1}$ solution under potentiodynamic polarization. The initial equilibrium potential was of 0.44 and 0.20 V the end potential. The potential scan rate was of $10.00\,mV\,s^{-1}$. The nucleation mechanism was investigated in the initial stages of cobalt electrodeposition under potentiostatic condition. All the electrochemical measurements were accomplished without solution agitation at 25 °C.

3. Results and discussions

3.1. Electrode characterization

A typical X-ray diffractogram of cathodes of spent Li-ion batteries is shown in Fig. 1. In comparison with Joint Committee on Powder Diffraction Standards (JCPDS), the cathode composition found was $LiCoO_2$, Co_3O_4, Al, and carbon [18–20]. The presence of Co_3O_4 in the cathode material results from the $LiCoO_2$ solid reaction that occurs during the charge–discharge cycles. In the discharge process when the amount of substance of lithium ions in $LiCoO_2$ reaches 0.50 it became in $Li_{0.5}CoO_2$. This compound is unstable and suffers chemical transformation. The reaction that occurs can be written by [21–23]:

$$Li_{0.5}CoO_2 \rightarrow 0.5LiCoO_2 + \tfrac{1}{6}Co_3O_4 + \tfrac{1}{6}O_2 \quad (3)$$

Carbon is used to increase the electrode electric conductivity. Aluminum constitutes the current collector. The X-ray diffractogram of the anode (Fig. 2) showed the presence of carbon, the active material, and Cu, the current collector [24]. The cathode and anode surface quantitative EDX measurements are shown

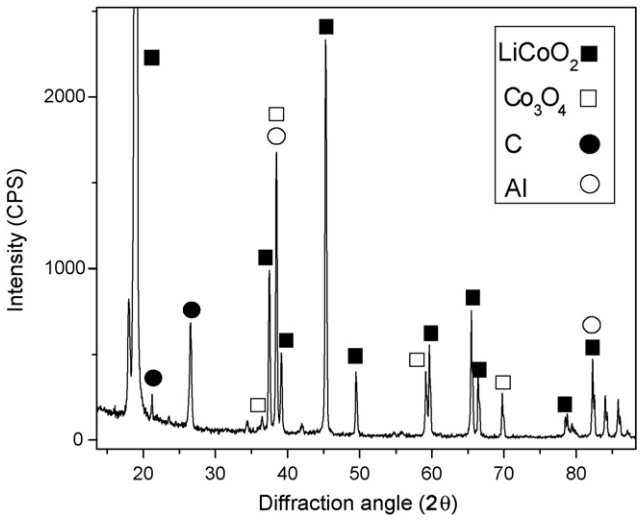

Fig. 1. Typical X-ray diffraction of cathode from spent Li-ion batteries.

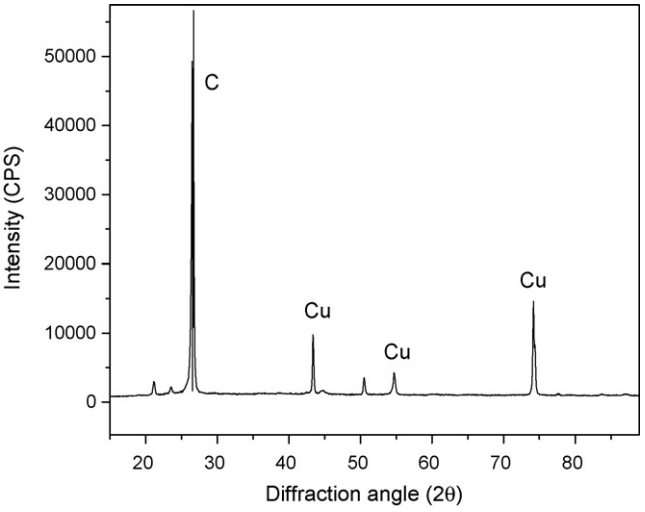

Fig. 2. Typical X-ray diffraction of anode from spent Li-ion batteries.

Table 1
Quantitative EDX of cathode and anode from spent Li-ion batteries

Chemical composition	Cathode (%)	Anode (%)
Cu	0.04	50.00
Co	99.70	1.90
C	0.20	46.10
P	0.06	2.00

in Table 1. The presence of copper as sludge in the cathode may be due to the migration of the ionic copper from the anode in the charge process. The presence of P is attributed to the $LiPF_6$ in the electrolyte. SEM micrographs of Li-ion battery electrodes are shown in Fig. 3. It is observed that the cathode (Fig. 3b) surface area is larger than that of the anode (Fig. 3a). The micrographs show that the cathode electrode is formed by crystal aggregates. Fig. 3b shows that the aggregates are formed by micropores, which allow the diffusion of the electrolyte to inner regions of the electrode, and microparticles, which assure a high specific area.

3.2. Potentiodynamic condition

Electrochemical recycling of cobalt from positive electrodes of spent Li-ion batteries was developed using potentiodynamic and potentiostatic conditions.

3.2.1. Formation of cobalt electrodeposits

Fig. 4 presents typical potentiodynamic curves of working electrodes in a solution with and without ionic cobalt at pH 5.40. Comparing the polarization curves, it is possible to see that ionic cobalt electrodeposition starts at −0.80 V, before the reduction of H^+. The increase in current density at cathodic potentials higher than −1.10 V is due to the increase in the detachment of hydrogen.

Successive scans show a decrease in the ionic cobalt electrodeposition potential (Fig. 4). After the first scan, electrodeposition happens on a cobalt. The potential decreases

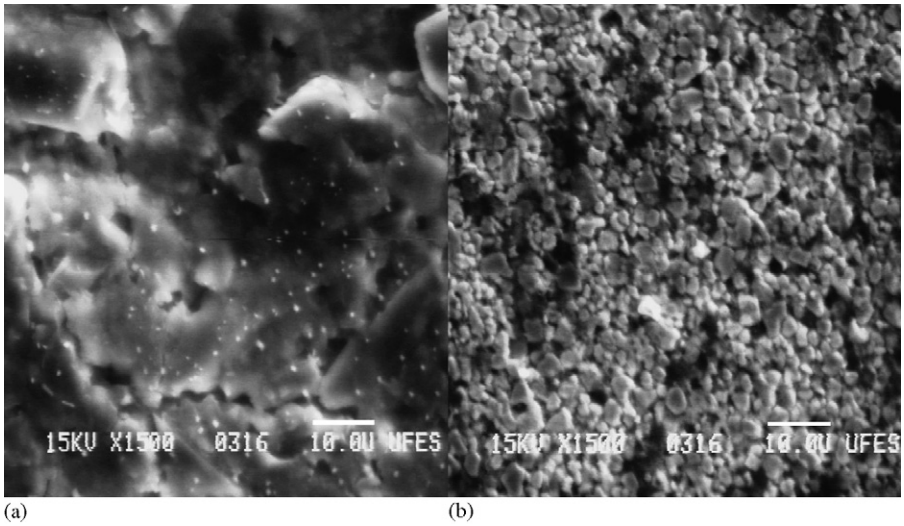

(a) (b)

Fig. 3. SEM of electrodes from spent Li-ion batteries: (a) anode; (b) cathode.

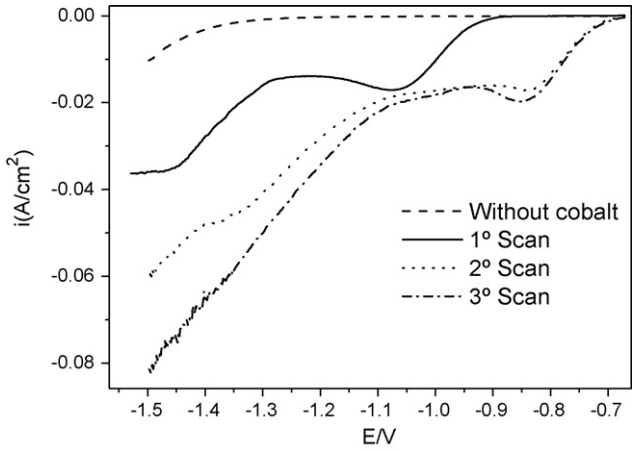

Fig. 4. Voltammetric curves with successive scan, cobalt concentration of 0.10 mol l^{-1}, pH 5.40, H_3BO_3 0.10 mol l^{-1} as buffer. The potential scan rate was 10.00 mV s^{-1}.

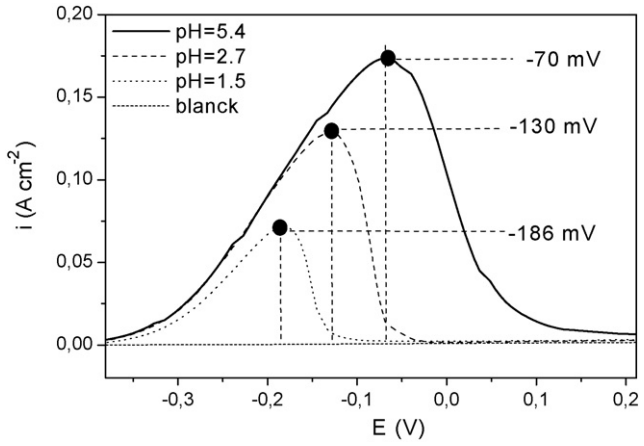

Fig. 6. Voltammetric curves for dissolution of cobalt electrodeposited with potential same to −1.00 V and charge density of 10.0 C cm^{-2} in: pH 5.40, 2.70, and 1.50. The electrolyte utilized in dissolution was H_2SO_4, pH 0.5.

because of the decrease in superficial free energy for ionic cobalt electrodeposition. The contribution of the current density for the reduction of H^+ increases with the decrease in pH. This behavior for solutions containing ionic cobalt at different pH values can be seen in Fig. 5.

3.2.2. Dissolution of cobalt electrodeposits

The electrodeposits formed at −1.00 V and charge density of 10.00 C cm^{-2} were dissolved in a H_2SO_4 0.50 mol l^{-1} solution by potentiodynamic technique (Fig. 6). It is observed that the ionic cobalt electrodeposition peak potential moves to more anodic regions with the increase in pH. The cobalt coating formed at pH 5.4 is more resistant to corrosion. In agreement with some authors' propositions, for pH above 4.00, cobalt electrodeposits form from $Co(OH)_2$ and the electrodeposits formed do not present adsorbed hydrogen [14–16]. The reactions can be written as follows:

$$Co_{(aq)}{}^{2+} + 2OH_{(aq)}{}^{-} \rightarrow Co(OH)_{2(s)} \quad (4)$$

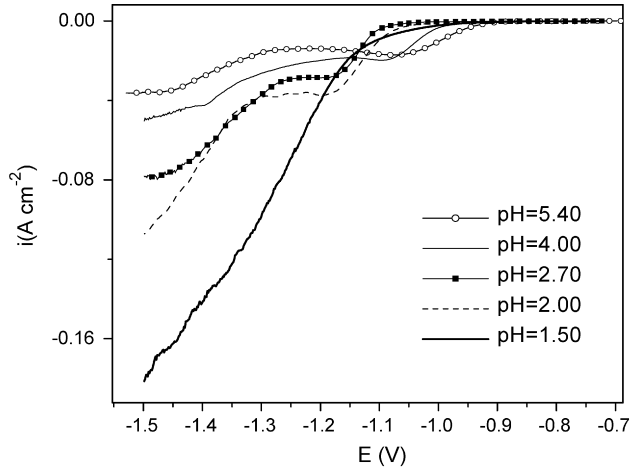

Fig. 5. Voltammetric curves for different pH, cobalt concentration of 0.10 mol l^{-1}, pH 5.40, 4.00, 2.70, 2.00, and 1.50, H_3BO_3 0.10 mol l^{-1} as buffer. The potential scan rate was 10.00 mV s^{-1}.

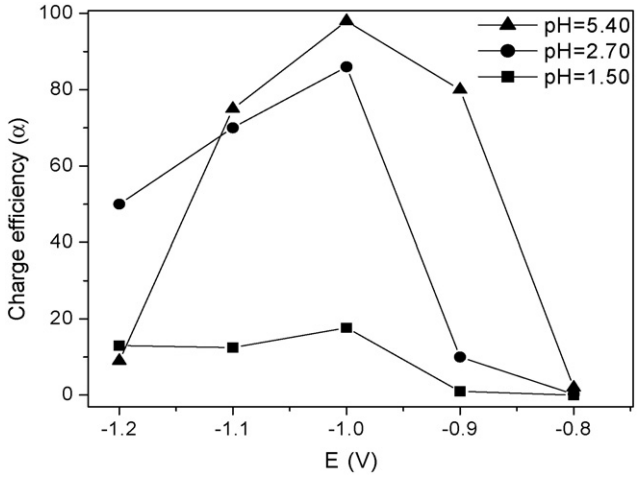

Fig. 7. Charge efficiency vs. electrodeposition potential, cobalt concentration of 0.10 mol l^{-1} in pH 5.40, 2.70 and 1.50 with H_3BO_3 0.10 mol l^{-1} as buffer, charge density of 10.0 C cm^{-2}.

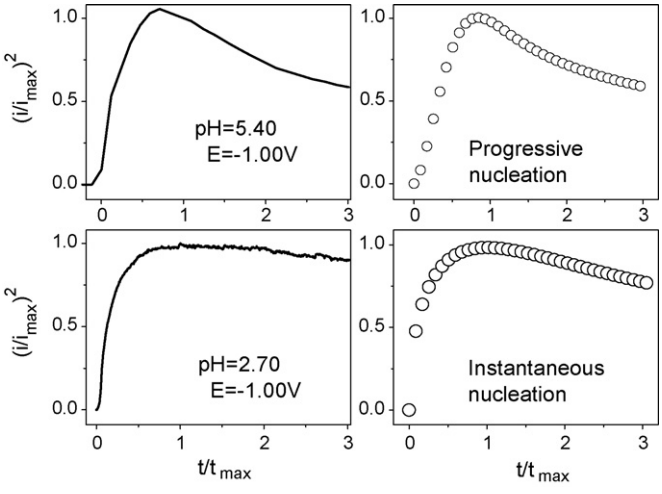

Fig. 8. Nucleation models for cobalt electrodeposited with potential same to −1.00 V and pH 5.40 and 2.70, cobalt concentration of 0.10 mol l^{-1} with H_3BO_3 0.10 mol l^{-1} as buffer.

$$Co(OH)_{2(s)} + 2e^- \rightarrow Co_{(s)} + 2OH_{(aq)}^- \quad (5)$$

For pH lower than 4.00, the electrodeposition of cobalt goes through an intermediate stage in which the adsorbed species is formed as an unstable compound. The subsequent reaction is the reduction of the adsorbed species to metallic cobalt. The cobalt deposit has adsorbed hydrogen. Cobalt electrodeposits with adsorbed hydrogen are less resistant to corrosion. This fact

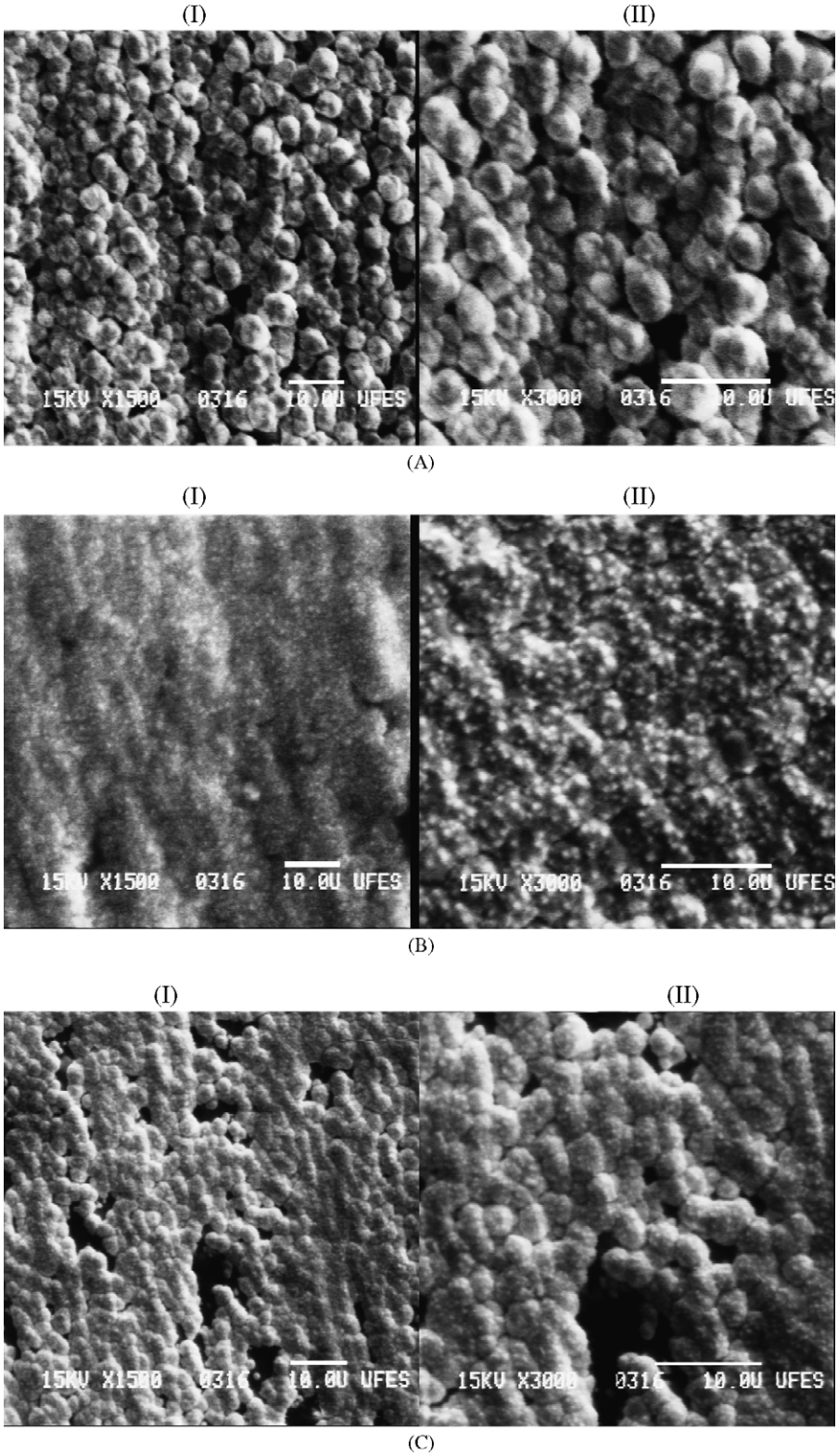

Fig. 9. SEM of cobalt electrodeposit at: (A) pH 5.40, (B) pH 2.70 and (C) pH 1.50. The potential applied of −1.00 V, charge density of 10.0 C cm^{-2}, cobalt concentration of 0.10 mol l^{-1} with H_3BO_3 0.10 mol l^{-1} as buffer, (I) 1500×, (II) 3000×.

may be associated to the inclusion of hydrogen in the crystalline structure of the electrodeposits. The reactions may be expressed as follows [15]:

$$Co_{(aq)}{}^{2+} + 2e^- \rightarrow Co_{(s)} \quad (6)$$

$$H_{(aq)}{}^{+} + Co + e^- \rightarrow CoH_{(ads)} \quad (7)$$

$$H_{(aq)}{}^{+} + CoH_{(ads)} + e^- \rightarrow Co_{(s)} + H_{2(ads)} \quad (8)$$

3.3. Potentiostatic condition

3.3.1. Charge efficiency

Fig. 7 presents the variation of charge efficiency with the electrodeposition potential for different pH values. Maximum charge efficiency is obtained at −1.00 V independently of pH conditions. The maximum charge efficiency is 96.90% at pH equal to 5.40. This high charge efficiency shows the small contribution of the H^+ reduction reaction. The maximum charge efficiency is equal to 86.20 and 17.20 for electrodeposition of ionic cobalt at pH 2.70 and 1.50, respectively. This result is expected because in this pH interval, ionic cobalt electrodeposition happens together with the reduction of H^+.

3.3.2. Nucleation mechanism

To study the initial stages of growth of the electrodeposits at pH 5.40 and 2.70 (high efficiency conditions), it was applied a potential of −1.00 V. Nucleation characterization is very difficult because the two types may take place in the same process. At pH 5.40, the electrodeposition data approaches the progressive nucleation (Fig. 8). According to this model, the nuclei are formed progressively and at a constant rate in the initial instants. The electrodeposits formed in this nucleation regime present a large nucleus size (three-dimensional growth). With the decrease in pH to 2.70, nucleation approaches the instantaneous nucleation model (Fig. 8), which has a quite high nucleus formation rate. Considering that the nuclei are formed simultaneously in this nucleation mechanism, the electrodeposits formed show a large amount of small nuclei. The mathematical nucleation proposed by Scharifker and Hills were investigated [25,26].

Instantaneous nucleation

$$\left(\frac{i}{i_{max}}\right)^2 = 1.945\left(\frac{t}{t_{max}}\right)^{-1}\left\{1 - \exp\left[-1.2564\left(\frac{t}{t_{max}}\right)\right]\right\}^2 \quad (9)$$

Progressive nucleation

$$\left(\frac{i}{i_{max}}\right)^2 = 1.2254\left(\frac{t}{t_{max}}\right)^{-1}\left\{1 - \exp\left[-2.3367\left(\frac{t}{t_{max}}\right)\right]\right\}^2 \quad (10)$$

Considering that the nuclei are formed simultaneously in this nucleation regime, the electrodeposits formed show a large amount of small nuclei. Microphotographs were made to analyze the deposit morphology.

3.3.3. SEM and EDX analyses

Electrodeposits obtained at −1.00 V with a charge density of 10.0 C cm^{-2} were measured by SEM. The electrodeposits formed at pH 5.40 (Fig. 9A) show a large grain size, evidencing that the nucleus growth follows the progressive nucleation model. At pH 2.70, the nuclei are smaller and in larger amount, which is in agreement with the instantaneous nucleation model (Fig. 9B). The deposits formed at pH 1.50 are very irregular and present holes (areas without deposition). The surface of the working electrode is partially covered with H_2 bubbles formed during the reduction reaction of H^+ ions. As a result, the area is not totally covered by electrodeposit layers, as can be seen in Fig. 9C. The EDX measurements of the electrodeposits obtained at −1.00 V with a charge density of 10.0 °C cm^{-2} showed that the surface is constituted of 100% cobalt.

4. Conclusions

According to X-ray diffraction, the composition of cathodes of spent Li-ion batteries is $LiCoO_2$, Co_3O_4, C, and Al. The Co_3O_4 present in the cathode results from the transformation of the active material ($LiCoO_2$). In the electrochemical recycling of cobalt, charge efficiency increases with increasing pH. The largest charge efficiency found was 96.90% at pH 5.40. The application of the nucleation models to the initial electrodeposition stages shows that at pH 5.40, the nuclei grow progressively (progressive nucleation). SEM showed a three-dimensional nucleus growth. With the decrease in pH to 2.70, the nucleation process becomes instantaneous (instantaneous nucleation).

For electrodeposits formed at −1.00 V the resistant to corrosion increase with the increase of pH. This fact is demonstrated by the decrease in adsorbed hydrogen in electrodeposits. In pH 5.4 the cobalt electrodeposition starts from $Co(OH)_2$. This mechanism does not result in hydrogen inclusion in the electrodeposits.

Acknowledgements

The authors acknowledge PRPPG-UFES and PETROBRAS for the financial support

References

[1] W.F. Howard, R.M. Spotnitz, J. Power Sources 165 (2007) 887.
[2] E. Plichta, S. Slane, M. Uchiyama, M. Salomon, D. Chua, W.B. Ebner, H.W. Lin, J. Electrochem. Soc. 136 (1989) 1865.
[3] S.S. Zhang, J. Power Sources 162 (2006) 1379.
[4] D. Aurbacha, Y. Talyosefa, B. Markovskya, E. Markevicha, E. Zinigrada, L. Asrafa, S.J. Gnanaraja, J.H. Kimb, Electrochim. Acta 50 (2004) 247.
[5] H. Sun, X. He, J. Ren, J. Li, C. Jiang, C. Wan, Eletrochem. Acta 52 (2007) 4312.
[6] UMICORE, Materials Technology Group, http://www.umicore.com (accessed on 14 April 2007).
[7] Y. Jyoko, S. Kashiwabara, Y. Hayashi, J. Electrochem. Soc. 144 (1997) 5.
[8] M. Palomar-Pardavé, B.R. Scharifker, E.M. Arce, M. Romero-Romo, Electrochim. Acta 50 (2005) 4736.

[9] S. Nakahara, S. Mahajan, J. Electrochem. Soc. 127 (1980) 283.
[10] L.H. Mendoza-Huizar, J. Robles, M. Palomar-Pardavé, J. Electroanal. Chem. 545 (2003) 39.
[11] D. Grujicic, B. Pesic, Electrochim. Acta 49 (2004) 4719.
[12] A. Vicenzo, P.L. Cavallotti, Electrochim. Acta 49 (2004) 4079.
[13] T. Osaka, Electrochim. Acta 42 (1997) 3015.
[14] S. Armyanov, Electrochim. Acta 45 (2000) 3323.
[15] J.T. Matsusshima, F. Trivinho-Strixino, E.C. Pereira, Electrochim. Acta 51 (2006) 1960.
[16] C. Lupi, M. Pasquali, A. Dell'Era, Waste Manage. 25 (2005) 215.
[17] S.P. Jiang, Y.Z. Chen, J.K. You, T.X. Chen, A.C.C. Tseung, J. Electrochem. Soc. 137 (1990) 3374.
[18] Joint Committee on Powder Diffraction Standars (JCPDS), Card No. JCPDS 16-427.
[19] Joint Committee on Powder Diffraction Standars (JCPDS), Card No. JCPDS 42-1467.
[20] Joint Committee on Powder Diffraction Standards (JCPDS), Card No. JCPDS 04-0787.
[21] O. Takahisa, K. Takashi, K. Takashi, T. Norio, S. Nao, S. Yuichi, S. Masahiro, S. Asako, J. Power Sources 146 (2005) 97.
[22] Y. Jun-ichi, B. Yasunori, K. Noriko, T. Hideyasu, E. Minato, O. Shigeto, J. Power Sources 119 (2003) 789.
[23] H.C. Liu, S.K. Yen, J. Power Sources 166 (2007) 478.
[24] Joint Committee on Powder Diffraction Standards (JCPDS), Card No. JCPDS 04-0836.
[25] G. Gunawardena, G. Hills, I. Montenegro, B. Scharifker, J. Electroanal. Chem. 138 (1982) 225.
[26] B. Scharifker, G. Hills, J. Electrochim. Acta 28 (1983) 879.